Science Advances
AAAS

advances.sciencemag.org/cgi/content/full/5/1/eaav5014/DC1

Supplementary Materials for

Ocean mesoscale mixing linked to climate variability

Julius J. M. Busecke* and Ryan P. Abernathey

*Corresponding author. Email: jbusecke@princeton.edu

Published 23 January 2019, *Sci. Adv.* **5**, eaav5014 (2019)
DOI: 10.1126/sciadv.aav5014

This PDF file includes:

1 Supplementary Materials

1.1 Discussion of velocity biases

The divergence correction does not affect the eddy properties - the small and short scale fluctuations as indicated by the almost identical eddy kinetic energy (EKE, not shown) between the corrected product and the uncorrected, also described in earlier work using this method (9). It does however introduce basinwide large scale biases, which are particularly pronounced during positive and negative phases of ENSO in the Pacific (fig. S1). The amplitude of these biases is quite small ($< 2cm/s$). But argued in the main text these small differences will change surface diffusivities considerably. This is particularly important since changes of the large scale circulation on the magnitude up to $1cm/s$ are certainly seen over a wide range of regions and timescales in the global ocean (e.g. Fig. 5E). Due to the large scale velocity bias, results from the tracer experiment might not reproduce realistic changes in diffusivity, particularly in the subtropical basins. While the large scale structure of interannual variations is not realistic, the amplitude is within the observed variability in surface currents (internannual and longer), as seen in fig. S1. It however, serves well as a sensitivity testbed in which the validity of the SMLT-derived diffusivities can be compared to an independent estimate of surface diffusivities, to gain confidence about applying SMLT to observed velocities.

1.2 Osborn-Cox Diffusivity based on Smoothing Operator

Nakamura (2001) (39) defines a scalar eddy diffusivity based on the tracer variance budget under generic Reynolds averaging. Our experiments use a convolution filter to apply spatial smoothing. Convolution is not a Reynolds average, so here we re-derive Nakamura's result for our filter-based approach, following the approach outlined in (42, 43).

Our smoothing operator, indicated by angle brackets, is defined by spatial convolution. For a scalar field $f(\mathbf{x}, t)$, the smoothed field is

$$\langle f \rangle = \int f(\mathbf{x}', t)\mathcal{G}(\mathbf{x} - \mathbf{x}'; \ell)d\mathbf{x} \tag{1}$$

We use a Gaussian Kernel in 2D, defined as

$$\mathcal{G}(\mathbf{x}; \sigma) = \frac{1}{2\pi\sigma^2}e^{-|\mathbf{x}|^2/2\sigma^2} \tag{2}$$

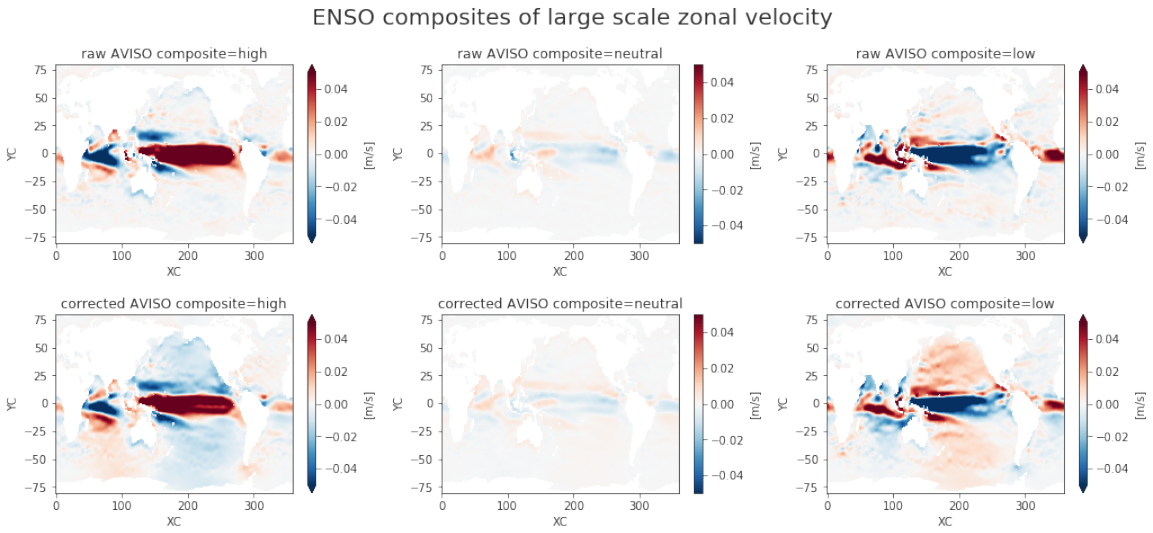

Fig. S1. Velocity bias introduced by divergence correction. The columns represent composite averages of high(left), neutral(center) and low(right) NINO3.4 indicies for the uncorrected - e.g. observed - velocities (upper) and the divergence corrected velocities (lower) used for the tracer experiment.

where σ is the standard deviation. Smoothing is not a Reynolds operator, because

$$\langle\langle f\rangle\rangle \neq \langle f\rangle \tag{3}$$

$$\langle f\ \langle g\rangle\rangle \neq \langle f\rangle\ \langle g\rangle \tag{4}$$

For second order statistics, we define the small-scale component via the operator τ, defined as

$$\tau(f,g) = \langle fg\rangle - \langle f\rangle\langle g\rangle \tag{5}$$

$$\tag{6}$$

The quantity $\tau(f,f)$ can be thought of as the small-scale variance, while $\langle f\rangle^2$ is the large-scale variance. They sum to give the total variance. The third-order fluctuation quantities are given by

$$\tau(f,g,h) = \langle f\ g\ h\rangle - \langle f\rangle\tau(g,h) - \langle g\rangle\tau(f,h) - \langle h\rangle\tau(f,g) - \langle f\rangle\langle g\rangle\langle h\rangle \tag{7}$$

Note that, since Reynolds averaging (e.g. time average) commutes with convolution, we can and do add time averaging to our smoothing operation with no change to the derivations below.

In many papers, the smoothing operation is applied to the momentum equation to derive a large-scale and small scale kinetic energy equation (42, 43) Here we apply it to the passive tracer equation

$$\partial_t\theta + \mathbf{u}\cdot\nabla\theta = \nabla\cdot\kappa\nabla\theta + s \tag{8}$$

where κ is the molecular diffusivity s is any (non-diffusive) source or sink. The flow is incompressible: $\nabla\cdot\mathbf{u} = 0$. Also, $\nabla\cdot\langle\mathbf{u}\rangle = 0$ The smoothed version is

$$\partial_t\langle\theta\rangle + \langle\mathbf{u}\rangle\cdot\nabla\langle\theta\rangle = -\nabla\cdot\tau(\mathbf{u},\theta) + \nabla\cdot\kappa\nabla\langle\theta\rangle + \langle s\rangle \tag{9}$$

The quantity $\tau(\mathbf{u},\theta)$ plays the role of the Reynolds flux. The total variance is $\langle\theta^2\rangle/2$. Using the τ operator, we can express it as the sum of a small-scale component and large-scale component. The small-scale tracer variance is given by

$$\frac{1}{2}\tau(\theta,\theta) = \frac{1}{2}(\langle\theta^2\rangle - \langle\theta\rangle^2) \tag{10}$$

To derive the tracer-variance equation, we start by multiplying (8) by θ and then smoothing. We get

$$\partial_t\frac{\langle\theta^2\rangle}{2} + \nabla\cdot\langle\mathbf{u}\frac{\theta}{2}\rangle = \nabla\cdot\kappa\frac{\langle\theta^2\rangle}{2} - \kappa\langle|\nabla\theta|^2\rangle \tag{11}$$

Next we multiply (9) by $\langle\theta\rangle$ to find

$$\partial_t \frac{\langle\theta\rangle^2}{2} + \langle\mathbf{u}\rangle\nabla\cdot\frac{\langle\theta\rangle^2}{2} = -\theta\nabla\cdot\tau(\mathbf{u},\theta) + \nabla\cdot\kappa\nabla\frac{\langle\theta\rangle^2}{2} - \kappa|\nabla\langle\theta\rangle^2| \tag{12}$$

In order to get to an equation for $\tau(\theta,\theta)/2$, we need to subtract (12) from (11). There is a bit of algebra to work out. First we note that

$$\langle\theta\rangle\nabla\tau(\mathbf{u},\theta) = \nabla\cdot\langle\theta\rangle\tau(\mathbf{u},\theta) - \tau(\mathbf{u},\theta)\cdot\nabla\langle\theta\rangle \tag{13}$$

Now we put all terms with a $\mathbf{u}$ in them on the left-hand side of the equation and simplify, using the third-order fluctuation definition. We obtain

$$\nabla\cdot\left[\langle\mathbf{u}\,\frac{\theta}{2}\rangle - \langle\theta\rangle\tau(\mathbf{u},\theta) - \langle\mathbf{u}\rangle\frac{\langle\theta\rangle^2}{2}\right] + \tau(\mathbf{u},\theta)\cdot\nabla\langle\theta\rangle \tag{14}$$

$$= \nabla\cdot\left[\langle\mathbf{u}\rangle\frac{\tau(\theta,\theta)}{2} + \frac{1}{2}\tau(\mathbf{u},\theta,\theta)\right] + \tau(\mathbf{u},\theta)\cdot\nabla\langle\theta\rangle \tag{15}$$

The terms proportional to κ give

$$\nabla\cdot\kappa\nabla\left(\frac{\langle\theta^2\rangle}{2} - \frac{\langle\theta\rangle^2}{2}\right) - \kappa\langle|\nabla\theta|^2\rangle + \kappa|\nabla\langle\theta\rangle|^2 \tag{16}$$

$$= \nabla\cdot\kappa\nabla\frac{\tau(\theta,\theta)}{2} - \kappa\tau[(\nabla\theta)^T,\nabla\theta] \tag{17}$$

Putting it all together, we find

$$\partial_t\frac{\tau(\theta,\theta)}{2} + \nabla\cdot\left[\langle\mathbf{u}\rangle\frac{\tau(\theta,\theta)}{2} + \frac{1}{2}\tau(\mathbf{u},\theta,\theta) - \kappa\nabla\frac{\tau(\theta,\theta)}{2}\right] + \tau(\mathbf{u},\theta)\cdot\nabla\langle\theta\rangle = -\kappa\tau((\nabla\theta)^T,\nabla\theta) \tag{18}$$

If we average over the whole domain and assume that the statistics are stationary in time, we are left with the balance

$$\int\tau(\mathbf{u},\theta)\cdot\nabla\langle\theta\rangle d\mathbf{x} = -\int\kappa\tau((\nabla\theta)^T,\nabla\theta)d\mathbf{x} \tag{19}$$

Because the right-hand side is negative definite, $\tau(\mathbf{u},\theta)$ must, on average, have the opposite sign to $\nabla\langle\theta\rangle$. That suggests that $\tau(\mathbf{u},\theta)$ can be represented via down-gradient diffusion.

Following (39), wecan try to separate the part of this flux associated with reversible processes from the down-gradient flux due to irreversible mixing. We let

$$\tau(\mathbf{u},\theta) = -(K_k + K_e)\nabla\langle\theta\rangle \tag{20}$$

Which are defined via

$$K_k = \frac{\partial_t\tau(\theta,\theta) + \nabla\cdot[\langle\mathbf{u}\rangle\tau(\theta,\theta) + \tau(\mathbf{u},\theta,\theta) - \kappa\nabla\tau(\theta,\theta)]}{2|\nabla\langle\theta\rangle|^2} \tag{21}$$

and

$$K_e = \kappa\frac{\tau((\nabla\theta)^T,\nabla\theta)}{|\nabla\langle\theta\rangle|^2} \tag{22}$$

or

$$K_m = \kappa\frac{\langle|\nabla\theta|^2\rangle}{|\nabla\langle\theta\rangle|^2} = K_e + \kappa \tag{23}$$

The quantity K_m is equivalent to the Osborn-Cox diffusivity of (9).

The main shortcoming of this approach is that our convolution operator does not commute precisely with differential operators on the sphere (44). This introduces small but nonzero residuals in the tracer variance equation.

1.3 Osborn-Cox cross frontal diffusivity using mulitple tracers

The spatial distribution of the scalar lateral surface diffusivities (K_{OC}) depends on the initial tracer field q_0, reflecting the anisotropy of the full diffusivity tensor projected onto the background gradient (9). We compute the diffusivities for 4 experiments with different initial tracer fields q_0

- $K_{OC,LAT}$ q_0 is a linear function of the latitude
- $K_{OC,PSI}$ q_0 is the mean horizontal streamfunction, based on the the mean dynamic topography from Aviso altimetry (9)
- $K_{OC,SST}$ q_0 is the mean climatological sea surface temperature (SST) (45)
- $K_{OC,SSS}$ q_0 is the mean climatological sea surface salinity (SSS) (45)

Each field is linearly interpolated onto the model grid.

A previous study using this methodology has focused on the spatial variability of the long-term mean (9). Using a different diagnostic but identical model setup (16) documented time variability in eddy diffusivities in the subtropical. In order

to resolve spatio-temporal variability, in this manuscript we combine some of the methods from both studies above: For each experiment (defined by the initial tracer field q_0), we compute two passive tracers (q) which are initialized identically and reset with equal and regular time intervals (390 days) but the reset phase of one tracer is shifted by half a reset interval, similar to (16). After each of the respective reset points the initial spin up phase (30 days) is removed due to the dominating role of the tendency term in the tracer variance budget (for details see (9, 16)). This results in a 5-dimensional array of diffusivities

$$K_{OC}\{longitude(lon), latitude(lat), time(ti), tracer(q), initial\,condition(q_0)\} \tag{24}$$

Results from experiments with several initial conditions mostly differ in terms of overall magnitude and spatial structure (fig. S2a), while temporal variability is very coherent across experiments on interannual and longer time scales, particularly in the subtropics of the Pacific (Fig. 2b).

This means that the temporal changes in diffusivity are driven by the velocity field. We compute a minimum diffusivity K_{min} across all four tracer experiments by selecting the lowest time-averaged diffusivity at each grid point. K_{min} is interpreted as the cross-frontal diffusivity (closely related to the minor axis of the diffusivity tensor), which is most relevant to identify mixing barriers (9). For simplicity, the rest of the manuscript will refer to K_{min} as K_{OC}; no results of single tracer experiments are used outside of the methods section. Details on the uncertainty of K_{min} are given below.

The root mean square error between tracers for each initial condition, defined as

$$RMSE_{tr,q0} = \sqrt{\langle (K_{OC}\{q, q_0\} - \langle K_{OC}\{q_0\}\rangle_q)^2\rangle_{ti,q_0}} \tag{25}$$

is minor compared to the mean diffusivities. The $RMSE_{q,q_0}$ (not shown) is mostly smaller than 2% of the local mean of K_{OC}. We quantify the uncertainty of K_{min} similar to Eq. 25 as

$$RMSE = \sqrt{\langle (\langle K_{OC}\rangle_q - \langle K_{OC}\rangle_{q,q_0})^2\rangle_{ti}} \tag{26}$$

The estimated uncertainty is smaller then 10% almost everywhere (fig. S2c). Most importantly the results presented in this dataset show very similar temporal evolution, indicating that the variability is indeed caused by the velocity field variability, and not the choice of initial condition.

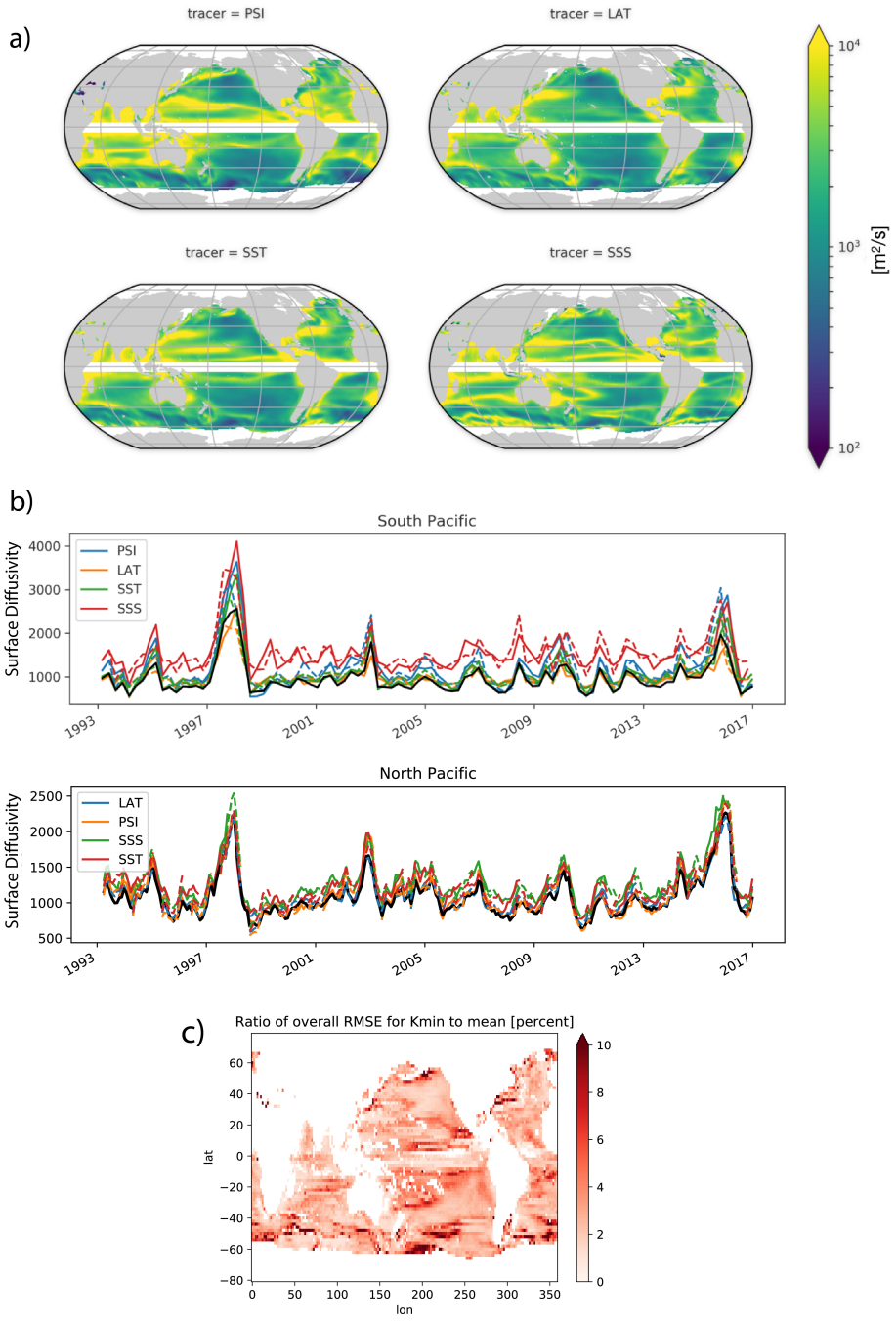

Fig. S2. Comparison of K_{OC} results for different initial conditions. a) Time mean surface diffusivity for each initial condition ('tracer') used in $[m^2/s]$. b) Example time series in the North and South Pacific boxes used in the main text (see Fig. 5). Colors indicate different initial conditions and solid and dashed line indicate the different tracers used for each initial condition (see text for details). c) The root mean square deviations corresponding to the two tracers used as well as the various initial conditions. For details see text.

2 Tracer variance budget

In order to use a diffusivity to parameterize the transport by mesoscale eddies, the main balance in the tracer variance budget (derived and explained in detail in Abernathey and Marshall 2013 (9)), needs to be between variance production and dissipation. To confirm that this balance holds we computed the full tracer variance budget for all initial conditions of the tracer experiment (described above) for 3 month averages, and in fact we see that for all tracers the balance holds both spatially (see maps in fig. S3 upper three rows) but also temporally as shown in the timeseries of dissipation and production, shown in the lower two rows of fig. S3, for values averaged in the previously used boxes in the North and South Pacific (see Fig. 5), where strong variability in the surface diffusivity is seen.

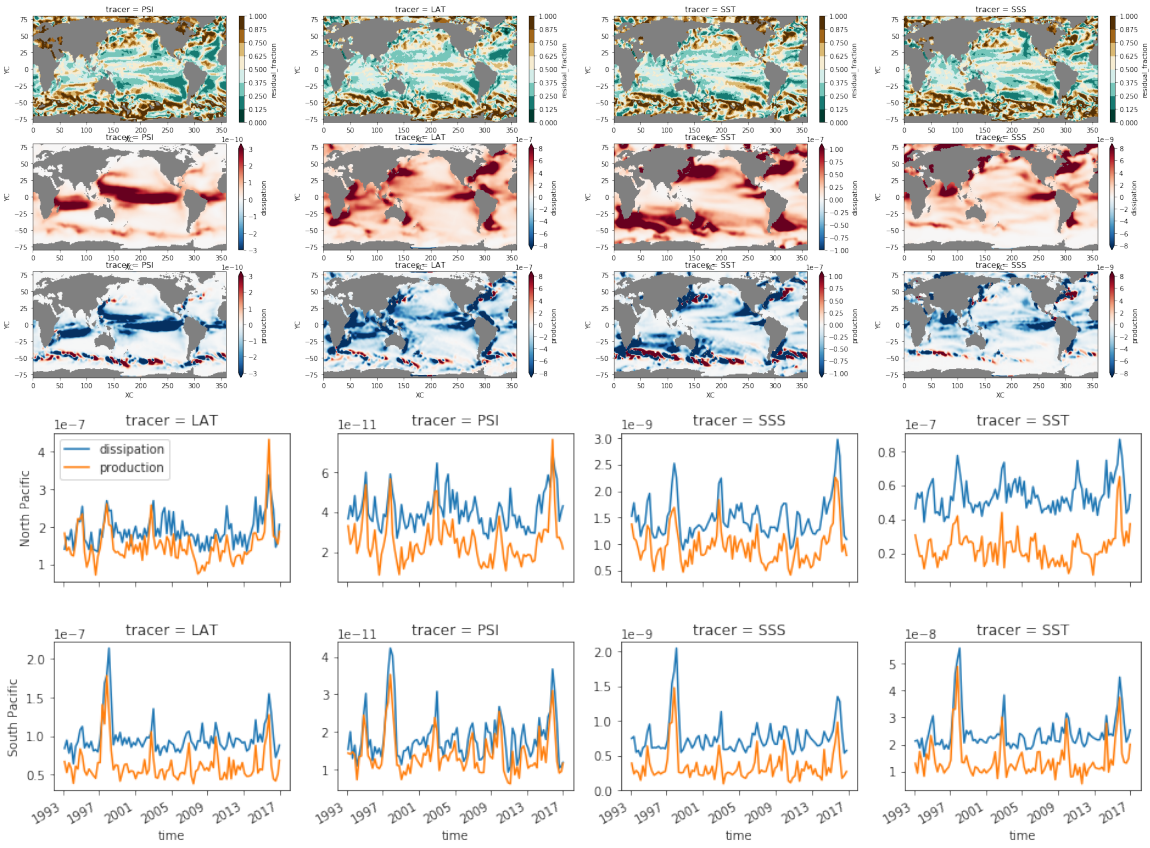

Fig. S3. Validation of tracer variance budget. Columns represent the 4 initial conditions used for the tracer experiment (see above for details). The first row shows the residual fraction defined as $\frac{|production+dissipation|}{|production|+|dissipation|}$. The second and third row show the dissipation and production term respectively as a long term average. The lower two rows show timeseries of both terms in the previously used example boxes (see e.g. Fig. 5), with the dissipation inverted. These show that for the large excursions in the Osborn-Cox diffusivity (described in main text), both terms increase(decrease), thus maintaining the balance and justifying the diffusive approach.